THE JOURNAL OF PHYSICAL CHEMISTRY C

Article

pubs.acs.org/JPCC

Distinctive Behavior of Photogenerated Electrons and Holes in Anatase and Rutile TiO_2 Powders

Akira Yamakata,*[,†,‡] Junie Jhon M. Vequizo,[†] and Hironori Matsunaga[†]

[†]Graduate School of Engineering, Toyota Technological Institute, 2-12-1 Hisakata, Tempaku, Nagoya 468-8511, Japan

[‡]Precursory Research for Embryonic Science and Technology (PRESTO), Japan Science and Technology Agency (JST), 4-1-8 Honcho Kawaguchi, Saitama 332-0012, Japan

Supporting Information

ABSTRACT: TiO_2 powders have been widely used for photocatalysts; however, why anatase shows higher activity than rutile has been a long-standing question. Here, we have elucidated the difference in the behavior of photogenerated electrons and holes by time-resolved visible to mid-IR absorption spectroscopy. In anatase TiO_2, a considerable number of free electrons survive longer than 1 ms, but they are deeply trapped within a few picoseconds in the case of rutile TiO_2. The longer lifetime of free electrons is responsible for the higher activity for reduction processes on anatase TiO_2. However, deep electron trapping in rutile TiO_2 elongates lifetime of holes and promotes multihole processes such as water oxidation. However, the low reactivity of deeply trapped electrons fails to increase the overall activity. These peculiar behaviors of electrons and holes are induced by defects on the powder particles and less sensitive to the physical properties such as particle size and specific surface area.

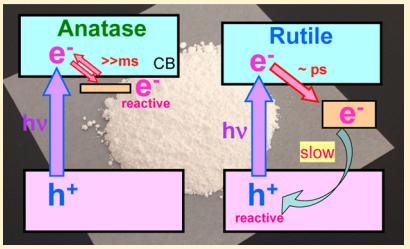

1. INTRODUCTION

Photocatalysts have attracted considerable attention due to their potential application to the water-splitting reaction and degradation of pollutants using solar energy. TiO_2 is one of the most often used materials for photocatalysts because it is nontoxic and chemically stable during photocatalytic reactions.[1−6] For TiO_2, anatase and rutile are the primary crystal structures, and their differences in photocatalytic activity have been well studied. In many photocatalytic reactions, anatase TiO_2 has a higher activity than rutile TiO_2. It is often proposed that this difference arises from the higher activity for the reduction of O_2, since O_2 anion radicals promote the oxidation of organic molecules.[7−9] Anatase TiO_2 also has a higher activity than rutile TiO_2 for water reduction reactions. However, in water oxidation, rutile TiO_2 has a much higher activity than anatase TiO_2.[7,10,11] Despite many reports discussing the differences in photocatalytic activity between anatase and rutile TiO_2, the principal reason for the difference in photocatalytic activity has not yet been fully elucidated. This fundamental information is indispensable, not only for the better understanding of the mechanism but also for the further development of highly efficient photocatalysts. The photocatalytic activity is determined by the energy states of the charge carriers as well as their behavior, so differences in the behavior of photogenerated electrons and holes should be investigated in detail.

Time-resolved absorption spectroscopy from the visible to mid-IR region is a powerful method of studying the behavior of photogenerated charge carriers. Especially in the visible to near-IR (NIR) region, holes and deeply trapped electrons give characteristic absorption peaks, so spectroscopy has been applied to investigate the behavior of deeply trapped electrons and holes in photocatalysts such as TiO_2,[12−17] α-Fe_2O_3,[18,19] and $LaTiO_2N$.[20] On the other hand, free electrons excited into the conduction band (CB) and shallowly trapped electrons in the midgap states have structureless broad absorptions in the mid-IR region.[21] These electrons are more reactive than deeply trapped electrons. Therefore, time-resolved measurements were performed to study the behavior of free and/or shallowly trapped electrons in TiO_2,[21−26] $NaTaO_3$,[27] GaN,[28] $LaTiO_2N$,[29] and $SrTiO_3$.[30−32] However, simultaneous measurements in the visible to mid-IR region (400 nm to 10 μm) that covers energies from 0.1 to 3.1 eV provide more useful information regarding not only the decay kinetics but also the energy states of trapped charge carriers. By using this method, we have elucidated that the behavior of photogenerated charge carriers on single crystals and powder particles are totally different.[31,32] Powders are richer in defects than single crystals,[33] and we found that most of charge carriers are trapped at the defects of the powder, but their lifetimes are much longer than that in defect-free single crystals. The defects are believed to accelerate the recombination but instead decelerate the recombination; i.e., defects on powder particles rather work positively to enhance the overall photocatalytic activity.

In the present work, we have elucidated the differences in the behavior of electrons and holes in polycrystalline anatase and rutile TiO_2 powders by time-resolved visible to mid-IR absorption spectroscopy. In the case of defect-free single crystalline TiO_2, several papers have been already reported that the recombination in anatase TiO_2 is slower than in rutile TiO_2.[34−36] However, we found that the behaviors of charge

Received: September 22, 2015
Revised: October 7, 2015
Published: October 8, 2015

DOI: 10.1021/acs.jpcc.5b09236
J. Phys. Chem. C 2015, 119, 24538−24545

carriers in defect-rich powders are totally different from those in single crystals (Figure S1).[32] Since photocatalysts are often used in powder form, the behaviors of charge carriers on the powder should be elucidated. We found that free electrons survive for longer than 1 ms in anatase TiO_2 powders, but they are deeply trapped within a few picosecond in the case of rutile TiO_2 powders. The deep electron trapping in rutile TiO_2 prevents recombination and elongates the lifetime of holes. These curious behaviors of charge carriers are less sensitive to the physical properties such as particle size and specific surface area and determine the distinctive photocatalytic activities of anatase and rutile TiO_2 powders. The detailed mechanism that determines the substantial difference in the photocatalytic activities of anatase and rutile TiO_2 powders will be discussed based on the behavior of charge carriers.

2. EXPERIMENTAL SECTION

Femtosecond time-resolved visible to mid-IR absorption measurements were performed using a pump−probe method based on a femtosecond Ti:sapphire laser system (Spectra-Physics, Solstice & TOPAS prime; duration 90 fs; repetition rate 1 kHz), as reported in our previous paper.[29] Briefly, a 350 nm pulse was utilized to excite the photocatalysts, and 22 000 cm^{-1} (455 nm), 14 300 cm^{-1} (700 nm), and 2000 cm^{-1} (5 μm) pulses were used for the probe light. In the mid-IR region, the probe light transmitted from the sample was detected by an MCT array detector (Infrared Systems Development Corporation, 128 Ch, 6000−1000 cm^{-1}). On the other hand, in the visible to NIR region, the diffuse reflected probe light from the sample was detected by a photomultiplier (Hamamatsu Photonics, H5784-03, 25 000−143 00 cm^{-1}). The NIR detection was limited up to 14 300 cm^{-1} by the sensitivity of the photomultiplier.

Microsecond time-resolved visible to mid-IR absorption measurements were performed by the custom-built spectrometers, as reported in our previous paper.[29] Briefly, in the mid-IR region (6000−1000 cm^{-1}), probe light emitted from an $MoSi_2$ coil was focused on the sample, and the transmitted light was introduced to a grating spectrometer. The monochromated light was detected by an MCT detector (Kolmar), and the output electric signal was amplified with an ac-coupled amplifier (Stanford Research Systems, SR560, 1 MHz). In the visible to NIR region (25 000−6000 cm^{-1}), a halogen lamp (50 W) and Si or InGaAs photodiodes were utilized for the probe light and detectors, and the experiments were performed in reflection mode. In each experiment, a 355 nm UV pulse from an Nd:YAG laser (Continuum, Surelite I; duration 6 ns; power 0.5 mJ; repetition rate 10−0.01 Hz) was used to excite the band gap of the photocatalysts. The time resolution of the spectrometers was limited to 1−2 μs by the bandwidth of the amplifier.

In the experiments, two anatase TiO_2 powders, TIO-1(A) (particle size: 21 nm; specific surface area: 73 m^2 g^{-1}) and TIO-10(A) (size: 15 nm; surface area: 100 m^2 g^{-1}), and two rutile TiO_2 powders, TIO-3(R) (size: 40 nm; surface area: 40 m^2 g^{-1}), and TIO-6(R) (size: 15 nm; surface area: 100 m^2 g^{-1}), supplied by the Catalysis Society of Japan were used without further treatment. Each TiO_2 powder was fixed on a circular CaF_2 plate with density of 3 mg cm^{-1} and placed in the closed IR cell. The measurements were performed either in vacuum or in the presence of O_2[22] or MeOH[23,24] vapor at room temperature.

3. RESULTS AND DISCUSSION

3.1. Behavior of Photogenerated Charge Carriers in Polycrystalline Anatase TiO_2 Powders. Transient absorption spectra of anatase TIO-10(A) induced by 355 nm laser pulse irradiation are shown in Figure 1a. After band gap

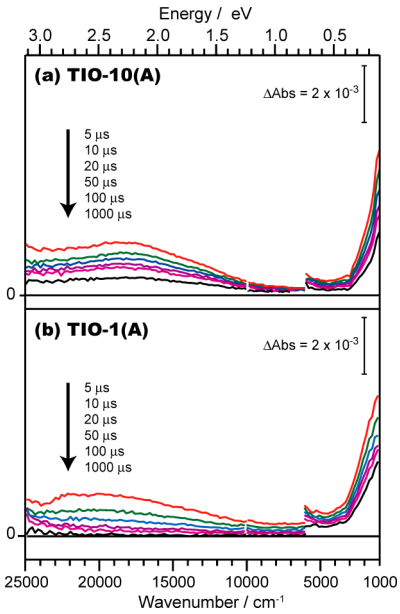

Figure 1. Transient absorption spectra of anatase TiO_2: (a) TIO-10(A) and (b) TIO-1(A) irradiated by UV laser pulses (355 nm, 6 ns duration, 0.5 mJ per pulse, and 5 Hz).

photoexcitation, a broad absorption was observed over the entire wavenumber region from 25 000 to 1000 cm^{-1} (400 nm to 10 μm) that could be divided into two features: a broad absorption from 25 000 to 13 000 cm^{-1} and another from 4000 to 1000 cm^{-1} of which the intensity increased with decreasing wavenumber. The monotonic absorption below 4000 cm^{-1} was assigned to the intraband transition of free electrons in CB or the direct transition of shallowly trapped electrons from the midgap states to the CB.[21] The depth of the electron trap was estimated to be smaller than 0.1 eV, as strong absorption was observed even at the low wavenumber limit of 1000 cm^{-1} (~0.1 eV).[21] This value is small enough for the thermal equilibrium with the free electrons. Therefore, both contributions of free and shallowly trapped electrons are involved in the absorption intensity below 4000 cm^{-1}. On the other hand, the broad absorption spanning from 25 000 to 13 000 cm^{-1} was ascribed to absorption by trapped electrons and/or holes.[21−26] The detailed assignment of the absorption is possible by observing the decay curves in the presence of reactant molecules.

The decay processes of transient absorption in TIO-10(A) were further examined in the presence and absence of O_2 and CH_3OH vapor. As shown in Figure 2, changes in the intensity at 2000, 18 000, and 22 000 cm^{-1} were measured. For the absorption at 2000 cm^{-1}, the decay was accelerated at 0−1 ms and decelerated after 1 μs by exposure to O_2 and CH_3OH vapor, respectively. Because these molecules capture electrons and holes, respectively, the results suggest that the absorption intensity at 2000 cm^{-1} reflects the number of electrons.[21,22,27,32] On the other hand, the absorption at 18 000 cm^{-1} exhibited a different trend: the absorption intensity increased with exposure to CH_3OH, suggesting that the intensity at 18 000

DOI: 10.1021/acs.jpcc.5b09236
J. Phys. Chem. C 2015, 119, 24538−24545

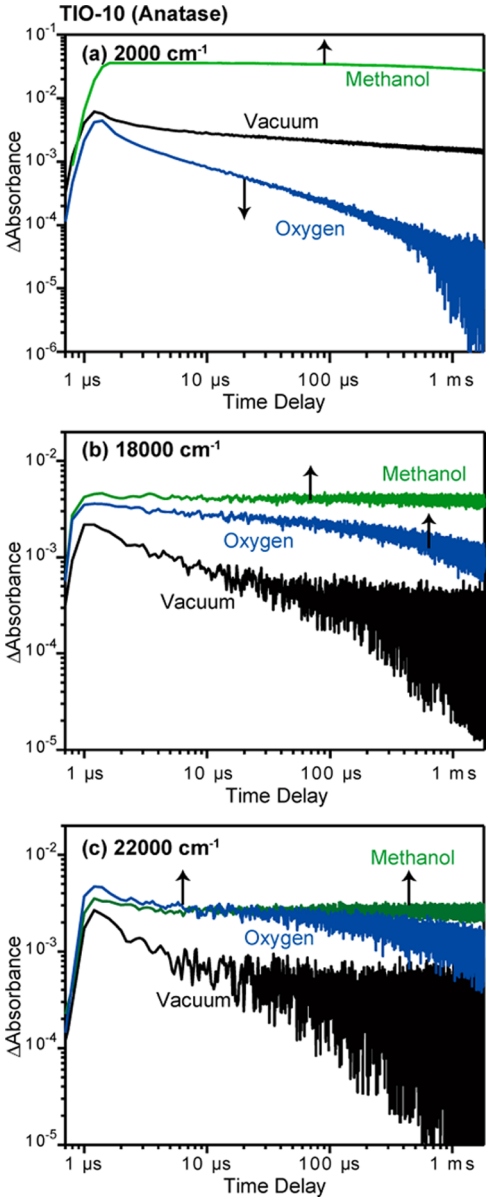

Figure 2. Decay curves of transient absorption by anatase TIO-10(A) irradiated by UV laser pulses (355 nm and 0.5 mJ per pulse) probed at 2000 (a), 18 000 (b), and 22 000 cm^{-1} (c) in a vacuum, 20 Torr of O_2, and CH_3OH.

cm^{-1} reflects the number of electrons. However, exposure to O_2 also increased the absorption intensity higher than that in a vacuum. This result suggests that the absorption at 18 000 cm^{-1} also reflects the number of holes; i.e., the intensity at 18 000 cm^{-1} reflects both electrons and holes. This assignment was justified by simple numerical simulations (see the Supporting Information Figure S3), and a similar behavior was observed for $SrTiO_3$ powders.[31]

For the decays at 22 000 cm^{-1}, the results were very similar to those at 18 000 cm^{-1}, and the intensity increased by exposure to either O_2 or CH_3OH (Figure 2c). These results confirm that the transient absorption at 22 000 cm^{-1} reflects the number of both electrons and holes. It has been reported that trapped holes and electrons in anatase exhibit very broad absorption at 450−550 nm (22 000−18 000 cm^{-1}) and 650−770 nm (15 000−13 000 cm^{-1}), respectively.[12−15] These absorption peaks are broad and overlapping, making it very difficult to distinguish them. Our results are consistent with the reports that the absorptions at 22 000 and 18 000 cm^{-1} arise from a mixture of trapped electrons and holes.

The same results were obtained on another anatase TiO_2 powder, TIO-1(A). The absorption intensity of TIO-1(A) at 18 000 cm^{-1} was slightly smaller than that of TIO-10(A) (Figure 1b), but the spectral shape was essentially the same with that of TIO-10(A). The similar decay curves were also observed at 2000, 18 000, and 22 000 cm^{-1} upon exposure to O_2 and CH_3OH (Figure S2). These results confirm that the energy states and the behaviors of charge carriers in TIO-10(A) and TIO-1 (A) are similar, indicating that they are less sensitive to the differences in physical properties such as particle size and specific surface area.

3.2. Behavior of Photogenerated Charge Carriers in Polycrystalline Rutile TiO_2 Powders. The behavior of photogenerated charge carriers in rutile TiO_2 powder was also examined by observing the transient absorption spectra after band gap excitation. As shown in Figure 3a, the spectral shape

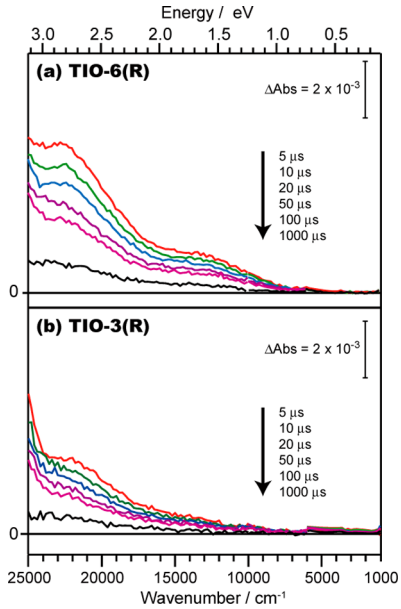

Figure 3. Transient absorption spectra of rutile TiO_2: (a) TIO-6(R) and (b) TIO-3(R) irradiated by UV laser pulses (355 nm, 6 ns duration, 0.5 mJ per pulse, and 5 Hz).

of TIO-6(R) was completely different from those observed for anatase TiO_2 powders (TIO-1(A) and TIO-10(A)), where the absorption intensity increased with increasing wavenumber from 1000 to 25 000 cm^{-1}. There were broad peaks at 22 000 cm^{-1} (455 nm) and 13 000 cm^{-1} (769 nm), but the absorption in the mid-IR region (<4000 cm^{-1}) was negligibly small compared to that of anatase TiO_2. These results confirm that the number of free or shallowly trapped electrons surviving in TIO-6(R) on the microsecond time scale was much smaller than that in anatase TiO_2.

The decay processes of photogenerated charge carriers in TIO-6(R) were further examined. As shown in Figure 4b, the intensity at 13 000 cm^{-1} increased within 1 μs after exposure to CH_3OH. This result suggests that the absorption at 13 000 cm^{-1} reflects the number of trapped electrons. However, exposure to O_2 gas did not change the intensity. This indicates that the trapped electrons, which cause the absorption at 13000 cm^{-1}, are not reactive with O_2.

DOI: 10.1021/acs.jpcc.5b09236
J. Phys. Chem. C 2015, 119, 24538−24545

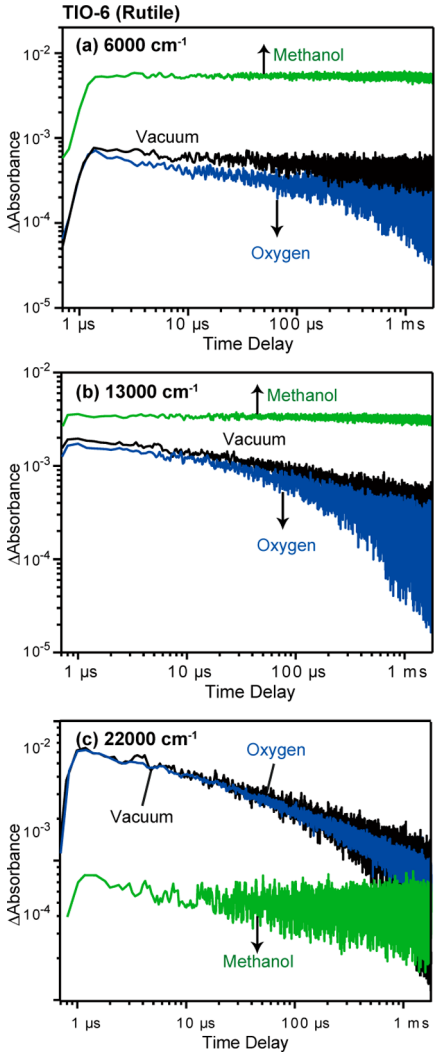

Figure 4. Decay curves of transient absorption by rutile TIO-6(R) irradiated by UV laser pulses (355 nm and 0.5 mJ per pulse) probed at 6000 (a), 13 000 (b), and 22 000 cm^{-1} (c) in a vacuum, 20 Torr of O_2, and CH_3OH.

For the absorption intensity at 22 000 cm^{-1} (Figure 4c), the opposite behavior was observed: it decreased within 1 μs after exposure to CH_3OH. This suggests that this absorption intensity reflects the number of holes. However, the intensity did not change upon exposure to O_2, which again confirms that the electrons generated in rutile TiO_2 are not consumed by O_2.

We further examined the reactivity of photogenerated electrons by observing the intensity change at 6000 cm^{-1} (Figure 4a) because the intensity at 2000 cm^{-1} was negligible. We expected that the absorption at 6000 cm^{-1} would reflect the number of more shallowly trapped electrons than those responsible for the absorption at 13 000 cm^{-1}. However, the intensity was not so affected by exposure to O_2 again, although the intensity increased within 1 μs after exposure to CH_3OH. Therefore, it is concluded that trapped electrons that survive for microseconds have less reactivity with the exposed O_2.

These results are consistent with those deduced from the shapes of the transient absorption spectra (Figure 3a), of which most of the electrons in the rutile were deeply trapped, so the reactivity was lower than that of free or shallowly trapped electrons generated in anatase TiO_2. The depth of the electron traps in rutile TiO_2 can be deduced from the transient absorption spectra observed at 18 000−7000 cm^{-1}. From the onset of absorption at 7000 cm^{-1} (~0.9 eV), the lower limit of the electron trap depth was estimated to be ~0.9 eV, suggesting that the electron traps in rutile TiO_2 are much deeper than those in anatase TiO_2 (<0.1 eV). In addition, similar results were obtained in another rutile powder, TIO-3(R) (Figure 3b and Figure S2), regardless of the differences in physical properties such as particle size and specific surface area as in the case of anatase TiO_2 powders.

3.3. Differences in the Behavior of Photogenerated Electrons and Holes in Anatase and Rutile TiO_2 Powders from Femtoseconds to Milliseconds. The decay process of photogenerated charge carriers in anatase and rutile TiO_2 powders was further investigated by comparing the decay curves obtained in Figures 2 and 4 as well as Figure S2. The transient absorptions at 2000, 13 000, and 22 000 cm^{-1} for each sample are summarized in Figure 5. It is evident from Figure 5a that the lifetime of free electrons in anatase TiO_2 is longer than that in rutile TiO_2, where the absorption intensity at 2000 cm^{-1} decreases in the order TIO-10(A) > TIO-1(A) ≫ TIO-3(R) > TIO-6(R). However, in the case of deeply trapped electrons at 13 000 cm^{-1} (Figure 5b), the order is opposite to that of free

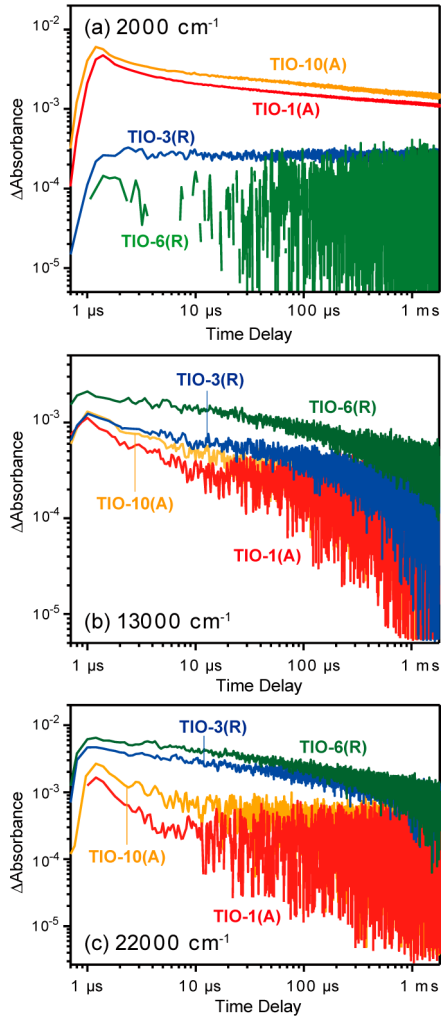

Figure 5. Decay curves of transient absorption by electrons and holes in TIO-1(A), TIO-10(A), TIO-3(R), and TIO-6(R), measured in a vacuum. The decay curves were probed at 2000 (a), 13 000 (b), and 22 000 cm^{-1} (c).

DOI: 10.1021/acs.jpcc.5b09236
J. Phys. Chem. C 2015, 119, 24538−24545

electrons, where the lifetime is longer in rutile than in anatase TiO_2: TIO-6(R) > TIO-3(R) > TIO-10(A) > TIO-1(A). For trapped holes at 22 000 cm^{-1}, the order is also opposite to that of free electrons, and the lifetime is longer in rutile TiO_2 than in anatase TiO_2. This is the same sequence as that of trapped electrons: TIO-6(R) > TIO-3(R) > TIO-10(A) > TIO-1(A) (Figure 5c). It is noted that the actual number of trapped electrons (holes) in anatase is much lower than that estimated from the absorption intensity at 13 000 cm^{-1} (22 000 cm^{-1}) because the holes (electrons) are involved in the absorption intensity at 13 000 cm^{-1} (22 000 cm^{-1}).

The initial decay process for free electrons in rutile TiO_2 was further examined using femtosecond time-resolved visible to mid-IR absorption spectroscopy. Figure 6 shows the intensity

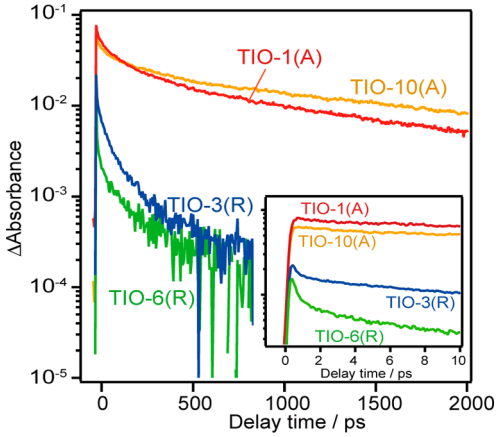

Figure 6. Decay curves of free electrons in polycrystalline anatase and rutile TiO_2 samples measured in vacuum at 2000 cm^{-1}.

changes at 2000 cm^{-1} for rutile TiO_2 (TIO-3(R) and TIO-6(R)) and anatase TiO_2 (TIO-1(A) and TIO-10(A)) excited by a 350 nm laser pulse. The number of free electrons in anatase TIO-1(A) and TIO-10(A) did not decrease very much from 0 to 10 ps but decreased rapidly in both rutile TIO-3(R) and TIO-6(R) from 0 to 2 ps. As a result, the number of free electrons surviving in TIO-1(A) and TIO-10(A) at 1000 ps is 100 times more than that in TIO-3(R) and TIO-6(R). In order to show the electron decay process more clearly, the normalized absorbance changes at 22 000, 14 300, and 2000 cm^{-1} are displayed in Figure 7. In TIO-1(A) and TIO-10(A), the rate of free-electron decay (2000 cm^{-1}) was comparable to that of trapped electrons (14 300 cm^{-1}) and holes (22 000 cm^{-1}). In TIO-3(R) and TIO-6(R), the decay rate of trapped electrons (14 300 cm^{-1}) is slightly slower than that of holes (22 000 cm^{-1}), but the rate of free-electron decay (2000 cm^{-1}) was significantly higher than that of trapped electrons and holes. These results confirm that the rapid decay of free electrons in rutile TiO_2 was not due to faster recombination but to rapid trapping at defects, because the decays of trapped electron and hole were much slower than that for the free electrons: the direct recombination of free electrons with holes cannot be a dominant process since the decay curve of free electrons is far from that of holes. When free electrons are deeply trapped at defects, the electron mobility decreases, thereby reducing the probability that the electrons will encounter with holes.[37−40] As a result, the lifetimes of holes in rutile TiO_2 becomes longer than in anatase TiO_2, in which more mobile free electrons are present.

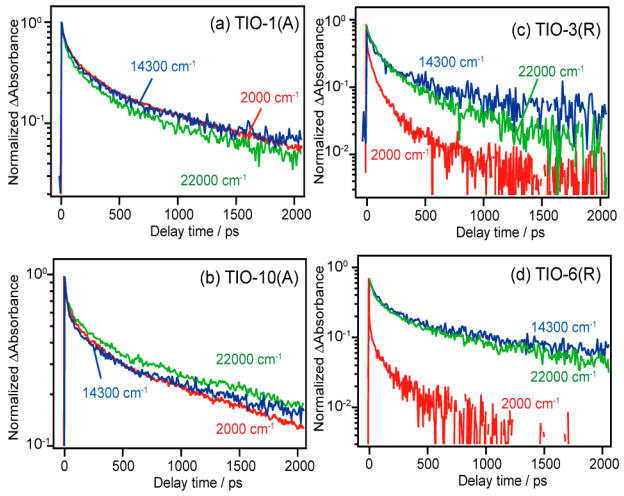

Figure 7. Normalized transient decays of electrons and holes in TIO-1(A), TIO-10(A), TIO-3(R), and TIO-6(R), measured in a vacuum and probed at 2000, 14 300, and 22 000 cm^{-1}.

3.4. Trapping of Charge Carriers and Effects on the Steady-State Photocatalytic Activity. The trapping of photogenerated charge carriers in TiO_2 particles has been studied by EPR,[41] FT-IR,[42−44] and photoluminescence (PL) spectroscopy.[45−48] In the case of anatase TiO_2 powder, it has been reported that Ti^{3+} at an oxygen vacancy acts as a deep electron trap, but these electron traps are limited in number, so most of the electrons are not deeply trapped.[41] Steady-state FT-IR measurements, which enable the detection of free electrons, support the EPR studies, indicating that free electrons have a longer lifetime and are the dominant carriers in anatase TiO_2.[42−44] PL measurements provide further information about the trapping of charge carriers.[45−48] It is proposed that photogenerated electrons are deeply trapped in rutile than in anatase TiO_2, since they show emission peak at 840 and ~500 nm, respectively.[45,46] However, PL measurement alone cannot categorically determine whether the red-shift is due to the deep trapping of electrons or holes. As a result, an alternate conclusion was proposed[47,48] where the NIR emission in rutile is not due to the deep trapping of electrons, but to deep trapping of holes although the peak was located at the same position (840 nm). Therefore, for the precise interpretation, other experimental supports are necessary.

Theoretical calculations provide a detailed picture of the defects on anatase and rutile TiO_2.[49−54] It is reported that excess electrons are trapped at the defects such as oxygen vacancy and Ti interstitials as Ti^{3+} with structural relaxation (polaron formation). The atomic displacement of the lattice via electron trapping is larger on rutile than on anatase, and hence the stabilization energy of the electron trapping in rutile defects is much larger than that of anatase. The detailed value depends on the calculation method, but the depths of the electron trap in anatase TiO_2 tend to be much shallower than in rutile TiO_2.[49−54] For example, they are estimated to be 0.8−1 and 0−0.2 eV for rutile and anatase, respectively.[52] As a result, electrons in rutile are heavily localized with hopping transport, but those in anatase are delocalized with conduction-band-like electron transport.[54] These reports support our experimental results where photogenerated electrons are deeply trapped in rutile defects and elongate the lifetime of holes.

The difference in photocatalytic activity between anatase and rutile TiO_2 powders can be reasonably explained by the results

DOI: 10.1021/acs.jpcc.5b09236
J. Phys. Chem. C 2015, 119, 24538−24545

obtained in this work. The higher photocatalytic activity for the reduction of anatase is often proposed to be responsibly due to the higher position of the CB in anatase TiO_2 than in rutile TiO_2. However, our experimental results clearly demonstrate that the difference in the depth of the electron trap is mainly responsible. In the case of anatase TiO_2, the electron traps are shallower than 0.1 eV, so these electrons are in equilibrium with free electrons. Furthermore, their lifetime is longer than 1 ms. Therefore, the electrons in anatase TiO_2 are highly reactive. However, in rutile TiO_2, the electron traps are much deeper (~0.9 eV), and most of the free electrons are quickly trapped at these defects within a few picoseconds. As a result, only a trace amount of free or shallowly trapped electrons survive in microsecond time scales. These results confirm that the difference in the reduction activities of anatase and rutile TiO_2 is caused by the longer lifetime of free electrons in anatase TiO_2 than that in rutile TiO_2.

In the case of photocatalytic oxidation, a clear difference was observed in the lifetime of holes, where it was much longer in rutile TiO_2 than in anatase TiO_2. The lifetime of holes is important for the higher activity, especially for multihole processes such as water oxidation; hence, rutile TiO_2 has a higher activity than anatase TiO_2. Under steady-state condition, photogenerated electrons are accumulated in the particles by filling the midgap states from deeper to shallower. These accumulated electrons in the shallow traps are reactive for water reduction, and hence rutile TiO_2 can split water in the absence of sacrificial reagents.[11] However, when the electrons are accumulated in the particles, the recombination with holes is accelerated.[55] As a result, the overall photocatalytic activity is not increased for many photocatalytic reactions. In the case of anatase TiO_2, photogenerated electrons are reasonably reactive even in the absence of electron accumulation; therefore, anatase TiO_2 exhibits higher activity in many photocatalytic reactions.

4. CONCLUSION

In this work, we have clearly elucidated the principal mechanism that determines the difference in photocatalytic activities of anatase and rutile TiO_2 powders. The biggest difference is the depth of the electron traps at powder defects, which were estimated to be <0.1 and >0.9 eV, respectively. In anatase TiO_2 particles, free and shallowly trapped electrons are in equilibrium and have a lifetime longer than 1 ms. These electrons are highly reactive, so anatase TiO_2 has a higher activity for photocatalytic reduction. On the contrary, free electrons in rutile TiO_2 are deeply trapped within a few picoseconds, and only a trace amount of free electrons survives for 1 ms. The deeply trapped electrons are less reactive, so rutile TiO_2 has a lower activity for reduction. However, this deep electron trapping acts to prevent recombination, extending the lifetimes of holes. The longer lifetime of holes promotes photocatalytic oxidation, especially for multihole processes such as water oxidation. Accumulation of electrons in rutile TiO_2 particles enables the water reduction, but it accelerates the recombination. As a result, the overall photocatalytic activity is not increased for many photocatalytic reactions. In anatase TiO_2, electrons and holes are both reactive, so anatase TiO_2 exhibits a higher photocatalytic activity than rutile TiO_2 in many photocatalytic reactions. These peculiar behaviors of charge carriers are induced by defects on the powder particles and less sensitive to the physical properties such as particle size and specific surface area. These insights offer lucid understanding of the catalytic mechanisms in anatase and rutile TiO_2 and can further be useful for the development of highly active photocatalysts based on TiO_2 materials.

■ ASSOCIATED CONTENT

Supporting Information

The Supporting Information is available free of charge on the ACS Publications website at DOI: 10.1021/acs.jpcc.5b09236.

Recombination kinetics in single-crystalline TiO_2, decay curves for anatase TIO-1(A) and rutile TIO-3(R) powders, numerical simulations, and decay curves in the picoseconds region (PDF)

■ AUTHOR INFORMATION

Corresponding Author

*E-mail: yamakata@toyota-ti.ac.jp (A.Y.).

Notes

The authors declare no competing financial interest.

■ ACKNOWLEDGMENTS

This work was supported by the PRESTO/JST program "Chemical Conversion of Light Energy". The authors acknowledge Grants-in-Aid for Specially Promoted Research (No. 23000009) and Basic Research (B) (No. 23360360) from the Ministry of Education, Culture, Sports, Science, and Technology (MEXT) of Japan. The authors also thank the Nippon Sheet Glass Foundation and the Nagai Foundation for Science and Technology.

■ REFERENCES

(1) Fujishima, A.; Honda, K. Electrochemical Photolysis of Water at a Semiconductor Electrode. *Nature* **1972**, *238*, 37−38.

(2) Kamat, P. V. Photochemistry on Nonreactive and Reactive (Semiconductor) Surfaces. *Chem. Rev.* **1993**, *93*, 267−300.

(3) Linsebigler, A. L.; Lu, G. Q.; Yates, J. T. Photocatalysis on TiO_2 Surfaces - Principles, Mechanisms, and Selected Results. *Chem. Rev.* **1995**, *95*, 735−758.

(4) Hagfeldt, A.; Gratzel, M. Light-induced Redox Reactions in Nanocrystalline Systems. *Chem. Rev.* **1995**, *95*, 49−68.

(5) Hoffmann, M. R.; Martin, S. T.; Choi, W. Y.; Bahnemann, D. W. Environmental Application of Semiconductor Photocatalysis. *Chem. Rev.* **1995**, *95*, 69−96.

(6) Ma, Y.; Wang, X.; Jia, Y.; Chen, X.; Han, H.; Li, C. Titanium Dioxide-Based Nanomaterials for Photocatalytic Fuel Generations. *Chem. Rev.* **2014**, *114*, 9987−10043.

(7) Ohno, T.; Haga, D.; Fujihara, K.; Kaizaki, K.; Matsumura, M. Unique Effects of Iron(III) Ions on Photocatalytic and Photoelectrochemical Properties of Titanium Dioxide. *J. Phys. Chem. B* **1997**, *101*, 6415−6419.

(8) Ohno, T.; Sarukawa, K.; Matsumura, M. Photocatalytic Activities of Pure Rutile Particles Isolated from TiO_2 Powder by Dissolving the Anatase Component in HF Solution. *J. Phys. Chem. B* **2001**, *105*, 2417−2420.

(9) Jia, J. G.; Ohno, T.; Matsumura, M. Efficient Dihydroxylation of Naphthalene on Photoirradiated Rutile TiO_2 Powder in Solution Containing Hydrogen Peroxide. *Chem. Lett.* **2000**, 908−909.

(10) Abe, R.; Sayama, K.; Domen, K.; Arakawa, H. A New Type of Water Splitting System Composed of Two Different TiO_2 Photocatalysts (Anatase, Rutile) and a IO^{3-}/I^- Shuttle Redox Mediator. *Chem. Phys. Lett.* **2001**, *344*, 339−344.

(11) Maeda, K. Direct Splitting of Pure Water into Hydrogen and Oxygen Using Rutile Titania Powder as a Photocatalyst. *Chem. Commun.* **2013**, *49*, 8404−8406.

(12) Bahnemann, D.; Henglein, A.; Lilie, J.; Spanhel, L. Flash-Photolysis Observation of the Absorption-Spectra of Trapped Positive

DOI: 10.1021/acs.jpcc.5b09236
J. Phys. Chem. C 2015, 119, 24538−24545

Holes and Electrons in Colloidal TiO_2. *J. Phys. Chem.* **1984**, *88*, 709−711.
(13) Bahnemann, D. W.; Hilgendorff, M.; Memming, R. Charge Carrier Dynamics at TiO_2 Particles: Reactivity of Free and Trapped Holes. *J. Phys. Chem. B* **1997**, *101*, 4265−4275.
(14) Yoshihara, T.; Katoh, R.; Furube, A.; Tamaki, Y.; Murai, M.; Hara, K.; Murata, S.; Arakawa, H.; Tachiya, M. Identification of Reactive Species in Photoexcited Nanocrystalline TiO_2 Films by Wide-wavelength-Range (400−2500 nm) Transient Absorption Spectroscopy. *J. Phys. Chem. B* **2004**, *108*, 3817−3823.
(15) Tamaki, Y.; Furube, A.; Murai, M.; Hara, K.; Katoh, R.; Tachiya, M. Direct Observation of Reactive Trapped Holes in TiO_2 Undergoing Photocatalytic Oxidation of Adsorbed Alcohols: Evaluation of the Reaction Rates and Yields. *J. Am. Chem. Soc.* **2006**, *128*, 416−417.
(16) Meekins, B. H.; Kamat, P. V. Role of Water Oxidation Catalyst IrO_2 in Shuttling Photogenerated Holes Across TiO_2 Interface. *J. Phys. Chem. Lett.* **2011**, *2*, 2304−2310.
(17) Wang, X. L.; Kafizas, A.; Li, X. O.; Moniz, S. J. A.; Reardon, P. J. T.; Tang, J. W.; Parkin, I. P.; Durrant, J. R. Transient Absorption Spectroscopy of Anatase and Rutile: The Impact of Morphology and Phase on Photocatalytic Activity. *J. Phys. Chem. C* **2015**, *119*, 10439−10447.
(18) Barroso, M.; Cowan, A. J.; Pendlebury, S. R.; Gratzel, M.; Klug, D. R.; Durrant, J. R. The Role of Cobalt Phosphate in Enhancing the Photocatalytic Activity of alpha-Fe_2O_3 toward Water Oxidation. *J. Am. Chem. Soc.* **2011**, *133*, 14868−14871.
(19) Barroso, M.; Mesa, C. A.; Pendlebury, S. R.; Cowan, A. J.; Hisatomi, T.; Sivula, K.; Gratzel, M.; Klug, D. R.; Durrant, J. R. Dynamics of Photogenerated Holes in Surface Modified Alpha- Fe_2O_3 Photoanodes for Solar Water Splitting. *Proc. Natl. Acad. Sci. U. S. A.* **2012**, *109*, 15640−15645.
(20) Singh, R. B.; Matsuzaki, H.; Suzuki, Y.; Seki, K.; Minegishi, T.; Hisatomi, T.; Domen, K.; Furube, A. Trapped State Sensitive Kinetics in $LaTiO_2N$ Solid Photocatalyst with and without Cocatalyst Loading. *J. Am. Chem. Soc.* **2014**, *136*, 17324−17331.
(21) Yamakata, A.; Ishibashi, T.; Onishi, H. Time-Resolved Infrared Absorption Spectroscopy of Photogenerated Electrons in Platinized TiO_2 Particles. *Chem. Phys. Lett.* **2001**, *333*, 271−277.
(22) Yamakata, A.; Ishibashi, T.; Onishi, H. Water- and Oxygen-Induced Decay Kinetics of Photogenerated Electrons in TiO_2 and Pt/TiO_2: A Time-Resolved Infrared Absorption Study. *J. Phys. Chem. B* **2001**, *105*, 7258−7262.
(23) Yamakata, A.; Ishibashi, T.; Onishi, H. Electron- and Hole-Capture Reactions on Pt/TiO_2 Photocatalyst Exposed to Methanol Vapor Studied with Time-Resolved Infrared Absorption Spectroscopy. *J. Phys. Chem. B* **2002**, *106*, 9122−9125.
(24) Yamakata, A.; Ishibashi, T.; Onishi, H. Effects of Water Addition on the Methanol Oxidation on Pt/TiO_2 Photocatalyst Studied by Time-Resolved Infrared Absorption Spectroscopy. *J. Phys. Chem. B* **2003**, *107*, 9820−9823.
(25) Heimer, T. A.; Heilweil, E. J. Direct Time-Resolved Infrared Measurement of Electron Injection in Dye-Sensitized Titanium Dioxide Films. *J. Phys. Chem. B* **1997**, *101*, 10990−10993.
(26) Yamakata, A.; Ishibashi, T.; Onishi, H. Microsecond Kinetics of Photocatalytic Oxidation on Pt/TiO_2 Traced by Vibrational Spectroscopy. *Chem. Phys. Lett.* **2003**, *376*, 576−580.
(27) Yamakata, A.; Ishibashi, T.; Kato, H.; Kudo, A.; Onishi, H. Photodynamics of $NaTaO_3$ Catalysts for Efficient Water Splitting. *J. Phys. Chem. B* **2003**, *107*, 14383−14387.
(28) Yamakata, A.; Yoshida, M.; Kubota, J.; Osawa, M.; Domen, K. Potential-Dependent Recombination Kinetics of Photogenerated Electrons in n- and p-Type GaN Photoelectrodes Studied by Time-Resolved IR Absorption Spectroscopy. *J. Am. Chem. Soc.* **2011**, *133*, 11351−11357.
(29) Yamakata, A.; Kawaguchi, M.; Nishimura, N.; Minegishi, T.; Kubota, J.; Domen, K. Behavior and Energy States of Photogenerated Charge Carriers on Pt- or CoO_x-loaded $LaTiO_2N$ Photocatalysts: Time-resolved Visible to mid-IR Absorption Study. *J. Phys. Chem. C* **2014**, *118*, 23897.
(30) Furuhashi, K.; Jia, Q.; Kudo, A.; Onishi, H. Time-Resolved Infrared Absorption Study of $SrTiO_3$ Photocatalysts Codoped with Rhodium and Antimony. *J. Phys. Chem. C* **2013**, *117*, 19101.
(31) Yamakata, A.; Yeilin, H.; Kawaguchi, M.; Hisatomi, T.; Kubota, J.; Sakata, Y.; Domen, K. Morphology-sensitive Trapping States of Photogenerated Charge Carriers on $SrTiO_3$ Particles Studied by Time-resolved Visible to Mid-IR Absorption Spectroscopy: the Effects of Molten Salt Flux Treatments. *J. Photochem. Photobiol., A* **2015**, DOI: 10.1016/j.jphotochem.2015.05.016.
(32) Yamakata, A.; Vequizo, J. J. M.; Kawaguchi, M. Behavior and Energy State of Photogenerated Charge Carriers in Single-Crystalline and Polycrystalline Powder $SrTiO_3$ Studied by Time-Resolved Absorption Spectroscopy in the Visible to Mid-Infrared Region. *J. Phys. Chem. C* **2015**, *119*, 1880−1885.
(33) Jupille, J.; Thornton, G. *Defects at Oxide Surfaces*; Springer: Switzerland, 2015.
(34) Xu, M. C.; Gao, Y. K.; Moreno, E. M.; Kunst, M.; Muhler, M.; Wang, Y. M.; Idriss, H.; Woll, C. Photocatalytic Activity of Bulk TiO_2 Anatase and Rutile Single Crystals Using Infrared Absorption Spectroscopy. *Phys. Rev. Lett.* **2011**, *106*, 138302.
(35) Luttrell, T.; Halpegamage, S.; Tao, J.; Kramer, A.; Sutter, E.; Batzill, M. Why is Anatase a Better Photocatalyst than Rutile?-Model Studies on Epitaxial TiO_2 Films. *Sci. Rep.* **2014**, *4*, 4043.
(36) Ozawa, K.; Emori, M.; Yamamoto, S.; Yukawa, R.; Yamamoto, S.; Hobara, R.; Fujikawa, K.; Sakama, H.; Matsuda, I. Electron-Hole Recombination Time at TiO_2 Single-Crystal Surfaces: Influence of Surface Band Bending. *J. Phys. Chem. Lett.* **2014**, *5*, 1953−1957.
(37) Nelson, J. Continuous-Time Random-Walk Model of Electron Transport in Nanocrystalline TiO_2 Electrodes. *Phys. Rev. B: Condens. Matter Mater. Phys.* **1999**, *59*, 15374−15380.
(38) Nelson, J.; Haque, S. A.; Klug, D. R.; Durrant, J. R. Trap-Limited Recombination in Dye-Sensitized Nanocrystalline Metal Oxide Electrodes. *Phys. Rev. B: Condens. Matter Mater. Phys.* **2001**, *63*, 205321.
(39) Barzykin, A. V.; Tachiya, M. Mechanism of Charge Recombination in Dye-Sensitized Nanocrystalline Semiconductors: Random Flight Model. *J. Phys. Chem. B* **2002**, *106*, 4356−4363.
(40) Tachiya, M.; Seki, K. Theory of Bulk Electron-Hole Recombination in a Medium with Energetic Disorder. *Phys. Rev. B: Condens. Matter Mater. Phys.* **2010**, *82*, 085201.
(41) Berger, T.; Sterrer, M.; Diwald, O.; Knozinger, E.; Panayotov, D.; Thompson, T. L.; Yates, J. T. Light-Induced Charge Separation in Anatase TiO_2 Particles. *J. Phys. Chem. B* **2005**, *109*, 6061−6068.
(42) Szczepankiewicz, S. H.; Moss, J. A.; Hoffmann, M. R. Slow Surface Charge Trapping Kinetics on Irradiated TiO_2. *J. Phys. Chem. B* **2002**, *106*, 2922−2927.
(43) Connor, P. A.; Dobson, K. D.; McQuillan, A. J. Infrared Spectroscopy of the TiO_2/Aqueous Solution Interface. *Langmuir* **1999**, *15*, 2402−2408.
(44) Sezen, H.; Buchholz, M.; Nefedov, A.; Natzeck, C.; Heissler, S.; Di Valentin, C.; Woll, C. Probing Electrons in TiO_2 Polaronic Trap States by IR-Absorption: Evidence for the Existence of Hydrogenic States. *Sci. Rep.* **2014**, *4*, 3808.
(45) Shi, J.; Chen, J.; Feng, Z.; Chen, T.; Lian, Y.; Wang, X.; Li, C. Photoluminescence Characteristics of TiO_2 and Their Relationship to the Photoassisted Reaction of Water/Methanol Mixture. *J. Phys. Chem. C* **2007**, *111*, 693−699.
(46) Wang, X.; Feng, Z.; Shi, J.; Jia, G.; Shen, S.; Zhou, J.; Li, C. Trap States and Carrier Dynamics of TiO_2 Studied by Photoluminescence Spectroscopy under Weak Excitation Condition. *Phys. Chem. Chem. Phys.* **2010**, *12*, 7083−7090.
(47) Knorr, F. J.; Mercado, C. C.; McHale, J. L. Trap-State Distributions and Carrier Transport in Pure and Mixed-Phase TiO_2: Influence of Contacting Solvent and Interphasial Electron Transfer. *J. Phys. Chem. C* **2008**, *112*, 12786−12794.

DOI: 10.1021/acs.jpcc.5b09236
J. Phys. Chem. C 2015, 119, 24538−24545

(48) Knorr, F. J.; Zhang, D.; McHale, J. L. Influence of $TiCl_4$ Treatment on Surface Defect Photoluminescence in Pure and Mixed-phase Nanocrystalline TiO_2. *Langmuir* **2007**, *23*, 8686−8690.
(49) Na-Phattalung, S.; Smith, M. F.; Kim, K.; Du, M. H.; Wei, S. H.; Zhang, S. B.; Limpijumnong, S. First-Principles Study of Native Defects in Anatase TiO_2. *Phys. Rev. B: Condens. Matter Mater. Phys.* **2006**, *73*, 125205.
(50) Finazzi, E.; Di Valentin, C.; Pacchioni, G. Nature of Ti Interstitials in Reduced Bulk Anatase and Rutile TiO_2. *J. Phys. Chem. C* **2009**, *113*, 3382−3385.
(51) Di Valentin, C.; Pacchioni, G.; Selloni, A. Reduced and n-Type Doped TiO_2: Nature of Ti^{3+} Species. *J. Phys. Chem. C* **2009**, *113*, 20543−20552.
(52) Mattioli, G.; Filippone, F.; Alippi, P.; Bonapasta, A. A. Ab Initio Study of the Electronic States Induced by Oxygen Vacancies in Rutile and Anatase TiO_2. *Phys. Rev. B: Condens. Matter Mater. Phys.* **2008**, *78*, 241201.
(53) Mattioli, G.; Alippi, P.; Filippone, F.; Caminiti, R.; Bonapasta, A. A. Deep versus Shallow Behavior of Intrinsic Defects in Rutile and Anatase TiO_2 Polymorphs. *J. Phys. Chem. C* **2010**, *114*, 21694−21704.
(54) Spreafico, C.; VandeVondele, J. The Nature of Excess Electrons in Anatase and Rutile from Hybrid DFT and RPA. *Phys. Chem. Chem. Phys.* **2014**, *16*, 26144−26152.
(55) Yamakata, A.; Ishibashi, T.; Onishi, H. Effects of Accumulated Electrons on the Decay Kinetics of Photogenerated Electrons in Pt/TiO_2 Photocatalyst Studied by Time-Resolved Infrared Absorption Spectroscopy. *J. Photochem. Photobiol., A* **2003**, *160*, 33−36.

DOI: 10.1021/acs.jpcc.5b09236
J. Phys. Chem. C 2015, 119, 24538−24545